# Flammability and Thermo-Oxidative Decomposition of Epoxy Resin Containing Ammonium Polyphosphate and Metallic Oxide

Lei Song[a]; Kun Wu[a]; Yun Wang[a]; Zhengzhou Wang[ab]; Yuan Hu[a]

[a] State Key Laboratory of Fire Science, University of Science and Technology of China, Anhui, PR China [b] School of Materials Science and Engineering, Tongji University, Shanghai, PR China

## PLEASE SCROLL DOWN FOR ARTICLE

Taylor & Francis
Taylor & Francis Group

# Flammability and Thermo-Oxidative Decomposition of Epoxy Resin Containing Ammonium Polyphosphate and Metallic Oxide

LEI SONG[1], KUN WU[1], YUN WANG[1], ZHENGZHOU WANG[1,2] and YUAN HU[1,*]

[1] *State Key Laboratory of Fire Science, University of Science and Technology of China, Anhui 230026, PR China*
[2] *School of Materials Science and Engineering, Tongji University, Shanghai 200092, PR China*

Cured epoxy resin (EP) composites containing Ammonium Polyphosphate (APP) and metallic oxide were prepared and characterized. The flame retardancy of the composites was studied using LOI, UL 94, cone calorimeter and Laser Raman spectroscopy, etc. The data of LOI, UL 94 and cone calorimeter show that APP is a good flame retardant for EP. The LOI value of the composite containing 20 wt% APP is as high as 38.0% and its UL 94 rating is raised to V-0. The addition of APP and $La_2O_3$ leads to the formation of char layer containing smaller carbonaceous microstructures compared with that of EP. Moreover, the thermo-oxidative decomposition of EP and its composites is characterized by dynamic FTIR.

**Keywords:** Epoxy resin, ammonium polyphosphate, thermal decomposition, flame retardancy

## 1 Introduction

Epoxy resins (EP) are widely used as coatings, adhesives and composites owing to their attractive characteristics mechanical and chemical properties. However, like most organic polymeric materials, EP is flammable and their application is limited. Therefore, many methods have been developed to improve the flame retardancy of EP. It is reported that epoxy resins can be modified with boron (1), phosphorus (2–5), silicone (6, 7), polyurethanes (8), melamine and melamine phenol-formaldehyde resin (9) and montmorillonite (10), etc. to enhance their flame retardancy. Among them, the use of phosphorus-containing compounds is promising. U. Braun et al. have done excellent work on the pyrolysis of neat epoxy resins containing phosphine oxide, phosphinate, phosphonate, and phosphate and the fire behaviour of their carbon fibre composites in order to investigate the influence of the oxidation state of the phosphorus on the fire retardancy of such materials (11).

Recently, intumescent flame retardant (IFR) has stimulated great attention in recent years because halogen-containing flame retardant materials produce a deal of smoke and toxic gases on burning. The conventional IFR system is composed of three parts: an acid source, a carbonization agent, and a blowing agent. The acid source is generally inorganic acid or precursor of the acid, for example, ammonium polyphosphate (APP). Carbonization agent is mainly polyhydric compound, such as pentaerythritol (PER) and starch. The compound used as a blowing agent can produce gases on heating, for instance, melamine (MEL), urea, etc. Bourbigot and his co-workers have done extensive studies on the APP IFR systems in polyolefins and reviewed the recent developments of IFR systems in great detail (12–15).

Due to the charring capacity of epoxy resin, it can be anticipated that addition of APP may be an effective and convenient approach for the flame retardancy of EP. Moreover, it is reported that some metallic compounds have synergistic effect on the flame retardancy of APP IFR system in polymers (16, 17). So, APP was combined with two metallic oxides (titanium dioxide ($TiO_2$) and lanthanum trioxide ($La_2O_3$)) to improve the flame retardant properties of EP composites further.

In this paper, diglycidyl ether of bisphenol A (DGEBA) was cured by m-Phenylenediamine, while EP/APP and EP/APP/metallic-oxide composites are prepared. The combustion characteristics of EP and IFR EP composites were studied using LOI, UL 94, cone calorimeter and Laser Raman Spectroscopy (LRS), etc. The thermo-oxidative decomposition of the EP and IFR EP composites were

---

*Address correspondence to: Yuan Hu, State Key Laboratory of Fire Science, University of Science and Technology of China, Anhui 230026, PR China; E-mail address: yuanhu@ustc.edu.cn
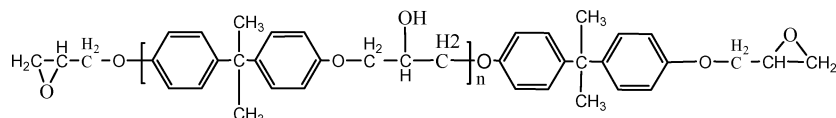
**DGEBA**
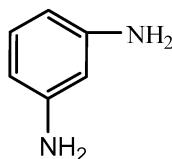
**m-Phenylenediamine**

**APP**

**Sch. 1.** Structure of DGEBA, m-Phenylenediamine and APP.
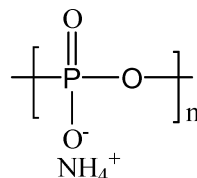
carried out by thermogravimetric analysis (TG) and dynamic Fourier transform infrared (FTIR), respectively.

## 2 Experimental

### 2.1 Materials

Diglycidyl ether of biphenol A (DGEBA, E-44) was purchased from Jiangsu Wuxi Resin Plant, China. m-Phenylenediamine is obtained from Shanghai Chemical Reagent Corporation, China. APP with an average degree of polymerization n > 1000 was purchased from Hangzhou JLS Flame Retardants Chemical Corporation. The structures of DGEBA, m-Phenylenediamine and APP are shown in Scheme 1. Metallic oxides were supplied by Shanghai Chemical Reagent Corporation.

### 2.2 Preparation of EP and IFR EP Composites

The base material used is a thermoset epoxy resin. The curing agent (m-Phenylenediamine) was mixed in an equivalent ratio (wt/wt: 11.8/100) with DGEBA. Then APP and metallic oxides were added into the matrix with different ratio. The mixtures were cured in a mould at 80°C for 2 h

and postcured at 150°C for 2 h to obtain cured specimens. The formulations of the samples are listed in Table 1.

### 2.3 Measurements

#### 2.3.1. *Limiting Oxygen Index*

LOI was measured according to GB/T 2406-1993. The apparatus used was an HC-2 oxygen index meter (Jiangning Analysis Instrument Company, China). The specimens used for the test were of dimensions $70 \times 6 \times 3$ mm.

#### 2.3.2. *UL-94 Testing*

The vertical test was carried out on a CFZ-2-type instrument (Jiangning Analysis Instrument Company, China) according to the UL 94 test standard. The specimens used were of dimensions $130 \times 13 \times 3$ mm.

#### 2.3.3. *Thermogravimetry (TG)*

Each sample was examined under air flow on a DTG-60H apparatus (Shimadzu Company) at a heating rate of 10°C/min.

#### 2.3.4. *Cone Calorimeter*

The combustion tests were performed on the cone calorimeter (Stanton Redcroft, UK) tests according to ISO 5660

**Table 1.** Formulations, LOI and UL 94 results of EP and IFR EP composites

| Sample Code | APP (wt%) | TiO$_2$ (wt%) | La$_2$O$_3$ (wt%) | LOI values (%) | UL 94 rating |
|---|---|---|---|---|---|
| EP | 0 | 0 | 0 | 25.5 ± 0.5 | N.R. |
| EPA10 | 10 | 0 | 0 | 30.0 ± 0.5 | N.R. |
| EPA20 | 20 | 0 | 0 | 38.0 ± 0.5 | V-0 |
| EPT-1 | 19 | 1 | 0 | 38.0 ± 0.5 | V-0 |
| EPT-2 | 18 | 2 | 0 | 38.5 ± 0.5 | V-0 |
| EPT-3 | 17 | 3 | 0 | 39.0 ± 0.5 | V-0 |
| EPL-1 | 19 | 0 | 1 | 39.0 ± 0.5 | V-0 |
| EPL-2 | 18 | 0 | 2 | 39.5 ± 0.5 | V-0 |
| EPL-3 | 17 | 0 | 3 | 39.5 ± 0.5 | V-0 |

standard procedures, with $100 \times 100 \times 3$ mm specimens. Each specimen was wrapped in an aluminum foil and exposed horizontally to 35 kW/m$^2$ external heat flux.

### 2.3.5. *Laser Raman Spectroscopy (LRS)*

The Raman spectra were recorded at an ambient temperature using a LABRAM-HR laser Raman spectrometer, with excitation provided in backscattering geometry by a 514.5 nm argon laser line.

### 2.3.6. *Dynamic Fourier Transform Infrared Spectra*

The samples were mixed with KBr powders, and the mixture were pressed into a tablet. The Fourier transform infrared (FTIR) spectra of samples were recorded using a Nicolet MAGNA-IR 750 spectrophotometer.

Dynamic FTIR spectra were recorded using above spectrophotometer equipped with a ventilated oven having a heating device. The temperature of the oven was raised at a heating rate of about $10°C$/ min. Dynamic FTIR spectra were obtained in situ during the thermo-oxidative decomposition of the samples.

## 3 Results and Discussion

### 3.1 LOI and UL 94 Rating

The LOI values and UL 94 testing results of EP and IFR EP composites are listed in Table 1. It can be seen that the LOI value increases sharply when APP is added into EP. The LOI value of the EP composite containing 20% APP (EPA20) is as high as 38.0% and its UL 94 rating is raised to V-0. However, pure EP can't pass any rating and its LOI value is just 25.5%. The above results show that APP is a good flame retardant for EP.

The effect of the two kinds of metallic oxides on the flame retardancy of the IFR EP composites is shown in Table 1. It can be seen that the LOI values change little with the increase of the loading of $TiO_2$ and $La_2O_3$. As we known that, the results of LOI is not very accurate and the uncertainty of LOI is $\pm 1$ in practice. From the data in Table 1, it can be concluded that the addition of $TiO_2$ and $La_2O_3$ have few effects on the LOI results of EP composites containing APP.

### 3.2 Cone Calorimeter

The heat release rate (HRR) curves of EP, EP/APP and EP/APP/$La_2O_3$ are shown in Figure 1.

EP is highly flammable. Associated data for EP are: Ignition time (IT) =100 s, Peak HRR=1704 kW/m$^2$.

The addition of APP in EP strongly decreases the HRR values and leads to an advance in the time to ignition compared to the virgin polymer. It is assumed that at the initial stage of heating, due to the reaction between APP and EP, the EP/APP composite (EPA20) decompose fast compared
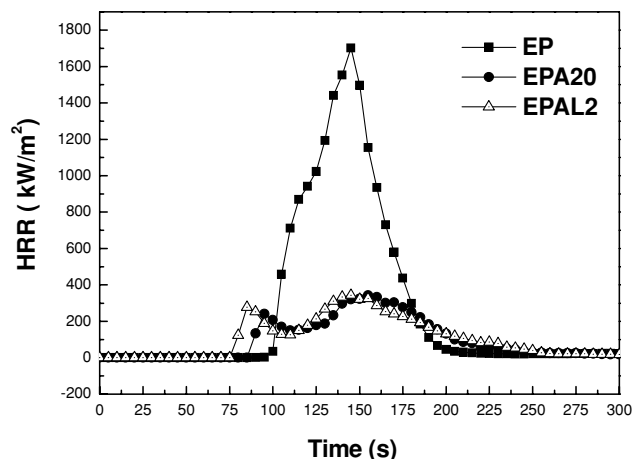


**Fig. 1.** HRR curves of EP, EPA20 and EPAL2.

with neat EP. Therefore, this makes the IT shortened and leads to the formation of a char. This char layer can prevent heat and oxygen from transferring into the matrix interior and protect the underlying material on burning as other papers mentioned (12–15). Associated data for EPA20 are: IT=85 s, Peak HRR= 344 kW/m$^2$.

The addition of $La_2O_3$ in EP/APP leads to a further advance in the time to ignition. Associated data for EPAL2 are: IT=75 s, Peak HRR= 344 kW/m$^2$. Moreover, from Figure 1, it is interesting to find that the EP has one single peak, whereas, there are two peaks for EP/APP and EP/APP/ $La_2O_3$.

The residues left after the cone calorimeter tests were taken photographs with a digital camera. Figure 2 are the photos of char residue of EP (a), EPA20 (b), EPAL2 (c). As for EP, there is no efficient intumescent char formed because EP almost decomposes completely. It can be seen that EPA20 and EPAL2 can form good and coherent intumescent char. The char is very black and thick.

### 3.3 Laser Raman Spectra

The structure of the intumescent char layer is very important for the flame retardant properties of IFR composites. Figure 3 shows the Raman spectra of residual char of EP, EPA20 and EPAL2 left after the cone calorimeter test. All spectra have two peaks at 1578 cm$^{-1}$ (labeled G) and 1346 cm$^{-1}$ (labeled D). The D peak represents the disordered graphite, such as the clusters of hexagonal rings. The G peak has been assigned to the ordered graphite which originates from the ordered hexagonal rings consisting of conducting $sp^2$-bonded carbon (18). It is reported that relative intensity ratio R of the D peak to the G peak is inversely proportional to an in-plane microcrystalline size and/or an in-plane phonon correlation length obtained from Raman spectroscopy (19). From Figure 3, it can be seen that the relative intensity ratio R is in the following order:
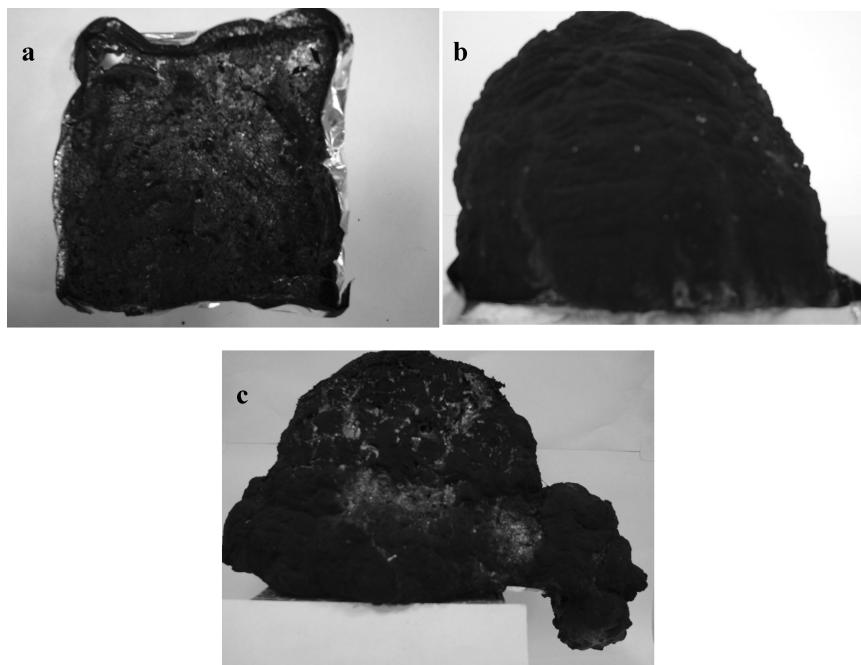
**Fig. 2.** Photos of residual char of EP (a), EPA20 (b) and EPAL2 (c).

EP < EPA20 < EPAL2. Therefore, the size of carbonaceous microstructures from the sample is in the following order: EP > EPA20 > EPAL2. Bourbigot and his coworkers found that higher protective shield efficiency was related to the smaller size of carbonaceous microstructures (20). It can be conclusion that the addition of APP and La$_2$O$_3$ lead to the formation of more compact char layer containing smaller carbonaceous microstructures. These results are in good agreement with the data of LOI, UL 94 test and cone calorimeter.

### 3.4 TG Analysis

The TG curves of APP, EP, EPA20 and EPAL2 are shown in Figure 4. The two decomposition steps of APP were previously reported in the literature (21). The first step, which begins around 270°C, is encouraged by the elimination of NH$_3$ and H$_2$O, leading to the formation of a crosslinked polyphosphoric acid (PPA). The second step, above the temperature of 520°C, corresponds to further decomposition of PPA.

In regard to EP, it begins to lose weight at about 280°C, and degrades almost completely below 640°C. From Figure 4, it can be seen that EPA20 shows a relatively weak thermal
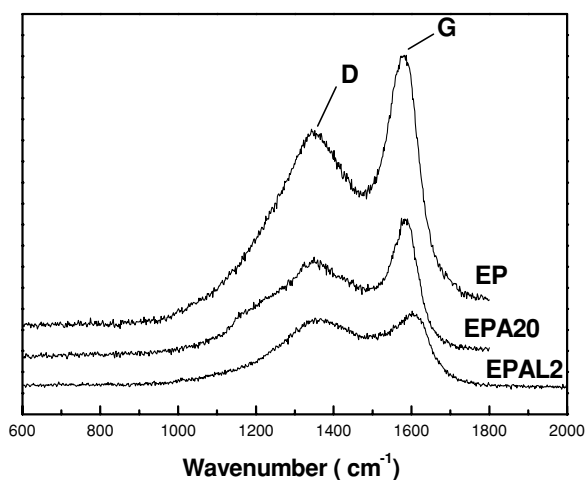


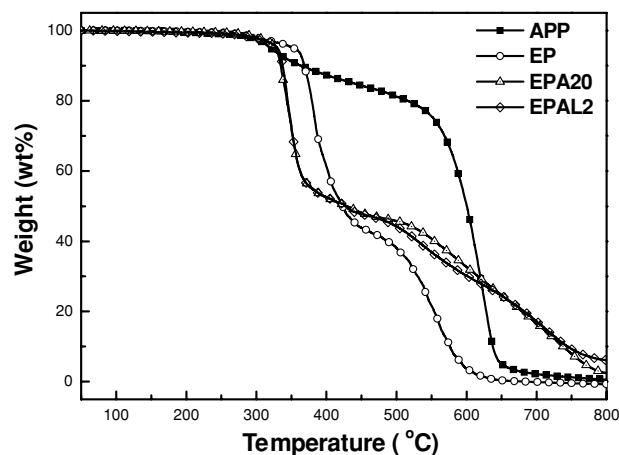**Fig. 3.** Raman spectra of residual char of EP, EPA20 and EPAL2.



**Fig. 4.** TG curves of APP, EP, EPA20 and EPAL2.

**Fig. 5.** FTIR spectra of EP at different pyrolysis temperature.



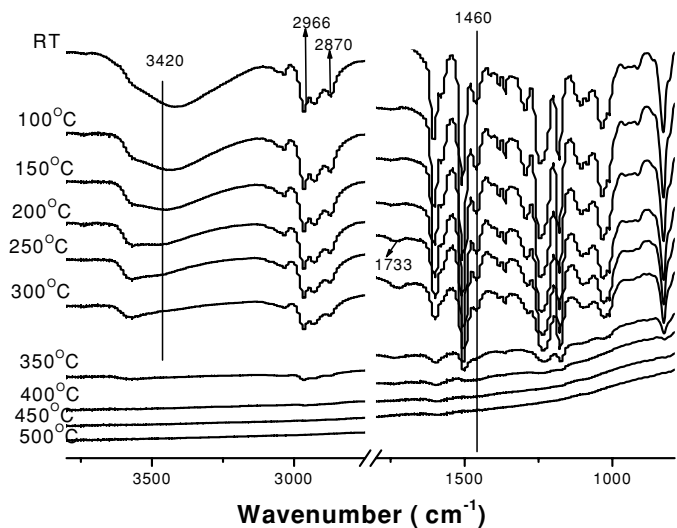**Fig. 6.** FTIR spectra of EPA20 at different pyrolysis temperature.

stability at lower temperature due to the reaction between APP and EP. This reaction leads to the formation of char. As a result, beyond the temperature of 423°C, EPA20 is more stable that EP. The residual weight of EPA20 at 800°C is 2.4%.

It also should be noted that the incorporation of $La_2O_3$ into EP/APP does not show significant effect on its thermo-oxidative decomposition at lower temperature, but the curve of EPAL2 shifts to higher temperature above 700°C. EPAL2 leaves 6.2% residual char at 800°C, which is much higher than of EP and EPA20. It can be drawn that the addition of $La_2O_3$ can improve the thermal stability of the char which can retard the weight loss rate of the composite at high temperatures.

### 3.5 Thermo-oxidative Decomposition

The details of the thermal oxidative behavior of materials can be revealed by the dynamic FTIR. Figures 5 and 6 show the dynamic FTIR spectra of EP and EPA20, respectively.

It can be seen from Figure 5 that the relative intensities of characteristic peaks for EP are almost not changeable below 200°C. However, with the temperature increase, the relative intensity of O—H absorption band around 3420 $cm^{-1}$ decreases gradually and nearly disappears completely at 400°C. The change of the band assigned to O—H group can be interpreted as the dehydration of the hydroxyl groups in EP (22, 23).

The changes of C—H absorption of aliphatic groups can be used to evaluate the thermal stability of samples during their thermal decomposition. From Figure 5, it is clear that the intensities of the bands at 2966 and 2870 $cm^{-1}$ ($CH_2$ and $CH_3$ asymmetric and symmetric vibrations) and 1460 $cm^{-1}$($CH_2$ and $CH_3$ deformation vibration of aliphatic group) decrease gradually, while the pyrolysis temperature up to 250°C is due to the thermal oxidative decomposi-
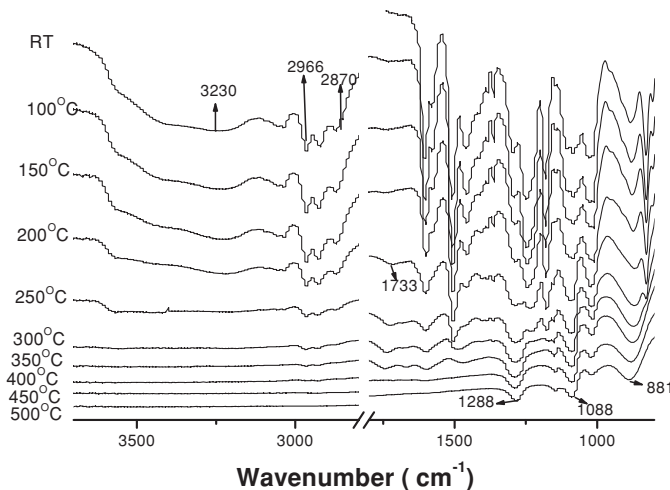
tion of EP main chains (24). This also can be testified by the appearance of the new peak at 1733 $cm^{-1}$ assigned to C=O at about 250°C (23). Between 300∼400°C, the main chains of EP are broken rapidly. When the temperature is above 450°C, all peaks nearly disappear, meaning that the EP resin decomposes completely.

Compared with EP, the thermal oxidative processe of EP/APP composite (EPA20) is much more complicated. Above 200°C the intensity of the strong and broad peak around 3230$cm^{-1}$ assigned to O-H and $NH_4^+$ begins to decrease (22, 23). This indicates that the composite begins to release water and ammonia due to the reaction between APP and EP. Moreover, the intensities of the peaks for $CH_2$ and $CH_3$ decrease gradually above 200°C and a new peak at 1733 $cm^{-1}$ assigned to C=O appears at about 250°C. The above results demonstrate that the main chains of EP are broken. It is interesting to find that between the range of 300 and 500°C, the shape of spectra show few change. It may be related with the formation of stable structures containing P—O—P and P=O (1288, 1088, 881 $cm^{-1}$) complexes (25).

The above data provides positive evidence of the flame retardant mechanism: APP can release the acid and react with EP at lower temperature to form a stable charred layer in the condensed phase. The char slows down heat and mass transfer between the gas and condensed phases and protects the underlying polymer on burning. These results are in agreement with the data of TG, LOI and UL 94.

### 4 Conclusions

In this work, APP used alone in EP can reach V-0 at the additive level 20%. The results of TG and cone calorimeter show that the presence of APP can promote the formation of intumescent charred layers and improve the thermal stability of EP at high temperature.

The addition of APP and $La_2O_3$ lead to the formation of more compact char layer containing smaller carbonaceous microstructures.

The thermo-oxidative decompositions of EP and EP/APP are also evaluated by dynamic FTIR. The results show that APP and EP can form a stable charred layer in the condensed phase and prevent the underlying polymeric from further decomposition during combustion.

## Acknowledgements

## References

1. Martin, C., Lligadas, G., Ronda, J.C., Galia, M. and Cadiz, V. (2006) *J. Polym. Sci. Pol. Chem.*, 44(21), 6332–6344.
2. Artner, J., Ciesielski, M., Walter, O., Doring, M., Perez, R.M., Sandler, Jan K.W., Altstadt, V. and Schartel, B. (2008) *Macromol. Mater. Eng.*, 293(6), 503–514.
3. Lin, C.H., Hwang, T.Y., Taso, Y.R. and Lin, T.L. (2007) *Macromol. Chem. Phys.*, 208(24), 2628–2641.
4. Zhang, X.H., Liu, F., Chen, S. and Qi, G.R. (2007) *J. Appl. Polym. Sci.*, 106(4), 2391–2397.
5. Lin, C.H., Feng, C.C. and Hwang, T.Y. (2007) *Eur. Polym. J.*, 43(3), 725–742.
6. Kumar, S. A., Denchev, Z. and Alagar, M. (2006) *Eur. Polym. J.*, 42(10), 2419–2429.
7. Chiu, Y.C., Liu, F.Y., Ma, C.C. M., Chou, I.C., Riang, L., Chiang, C.L. and Yang, J.C. (2008) *Thermochim. Acta*, 473(1–2), 7–13.
8. Wu, C.S., Liu, Y.L. and Chiu, Y.S. (2002) *J. Appl. Polym. Sci.*, 85(10), 2254–2259.
9. Shieh, J.Y. and Wang, C.S. (2001) *Polymer*, 42(18), 7617–7625.
10. Kaya, E., Tanoglu, M. and Okur, S. (2008) *J. Appl. Polym. Sci.*, 109(2), 834–840.
11. Braun, U., Balabanovich, A.I., Schartel, B., Knoll, U., Artner, J., Ciesielski, M., Doring, M., Perez, R., Sandler, J.K.W., Altstadt, V., Hoffmann, T. and Pospiech, D. (2006) *Polymer*, 47, 8495–8508.
12. Le Bras, M., Bourbigot, S., Delporate, C., Siat, C. and Le Tallec, Y. (1996) *Fire Mater.*, 20(4), 191–203.
13. Almeras, X., Le Bras, M., Hornsby, P., Bourbigot, S., Marosi, G., Keszei, S. and Poutch, F. (2003) *Polym. Degrad. Stab.*, 82(2), 325–331.
14. Almeras, X., Le Bras, M., Poutch, F., Bourbigot, S., Marosi, G. and Anna, P. (2003) *Macromol. Symp.*, 198, 435–447.
15. Bourbigot, S., Le Bras, M., Duquesne, S. and Rochery, M. (2004) *Macromol. Mater. Eng.*, 289(6), 499–511.
16. Lewin, M. and Endo, M. (2003) *Polym. Adv. Technol.*, 14(1), 3–11.
17. Soares, S., Camino, G. and Levchik, S. (1998) *Poly. Degrad. Stab.*, 62, 25–31.
18. Robertson, J. (2002) *Mat. Sci. Eng. R.*, 37(4–6), 129–281.
19. Tuinstra, F. and Koenig, J. L. (1970) *J. Chem. Phys.*, 53(3), 1126–1130.
20. Bourbigot, S., Le Bras, M., Delobel, R. and Tremillon, J.M. (1996) *J. Chem. Soc. Faraday Trans.*, 92(18), 3435–3444.
21. Camino, G., Grassie, N. and McNeill, I.C. (1978) *J. Polym. Sci., Polym. Chem. Ed.*, 16, 95–106.
22. Xiao, J.F., Hu, Y., Yang, L., Cai, Y.B., Song, L., Chen, Z.Y. and Fan, W.C. (2006) *Polym. Degrad. Stab.*, 91(9), 2093–2100.
23. Wang, Z.Z., Wu, G.S., Hu, Y., Ding, Y., Hu, K.L. and Fan, W.C. (2002) *Polym. Degrad. Stab.*, 77(3), 427–434.
24. Saihi, D., Vroman, S., Giraud, S. and Bourbigot, S. (2006) *React. Funct. Polym.*, 66(10), 1118–1125.
25. Wu, Q., Lv, J.P. and Qu, B.J. (2003) *Polym. Int.*, 52(8), 1326–1331.